Parks, G.A., 1972. Free energies of formation and aqueous solubilities of aluminum hydroxides and oxide hydroxides at 25°C. Am. Mineral., v. 57, p. 1163–1189.

Raupach, M., 1963. Solubility of simple aluminum compounds expected in soils, I. Hydroxides and oxyhydroxides. Australian J. Soil Res., v. 1, p. 28–35.

Russell, A.S., Edwards, J.D., and Taylor, C.S., 1955. Solubility and density of hydrated alumina in NaOH solutions. J. Metals, v. 7, p. 1123–1128.

Sanjuan, B., and Michard, G., 1987. Aluminum hydroxide solubility in aqueous solutions containing fluoride ions at 50°C. Geochim. Cosmochim. Acta, v. 51, p. 1823–1831.

Sato, T., 1954. Hydrolysis of sodium aluminate solution. XIII. Effect of decomposition temperature [in Japanese]. J. Chem. Soc. Japan., Ind. Chem. Sec. v. 57, p. 805–808.

Tanger, J.C., and Helgeson, H.C., 1988. Calculation of the thermodynamic and transport properties of aqueous species at high pressures and temperature: I. Revised equation of state for the standard partial molal properties of ions and electrolytes. Am. J. Sci., in press.

Taylor, C.S., Tosterud, M., and Edwards, J.D., 1927. The physical chemistry of aluminum. Aluminum Company of America Report R-95, 75 p.

Thompson, L.C.A., 1955. The equilibrium of aluminum hydroxide, uranium peroxide dihydrate and urano-uranate hydrate in acidic and alkaline media at 25°C. Unpublished dissertation, Wayne State University, Detroit, Michigan, 69 p.

Van Straten, H.A., 1984. Formation of solid phases from supersaturated aluminate solutions (Ph.D. thesis). University of Utrecht, Holland, 153 p.

Van Straten, H.A., and de Bruyn, P.L., 1984. Precipitation from supersaturated aluminate solutions. II. Role of temperature. J. Colloid Interface Sci., v. 102, p. 260–277.

Van Straten, H.A., Holtkamp, B.T.W., and de Bruyn, P.L., 1984. Precipitation from supersaturated aluminate solutions. I. Nucleation and growth of solid phases at room temperature. J. Colloid Interface Sci., v. 98, p. 342–362.

Wefers, K., 1967. Zur chemischen Technologie des Bauxitaufschlusses. Teil 1: Das System Na_2O–Al_2O_3–H_2O. Metall., v. 25, no. 5, p. 422–431.

The Thermodynamic Properties of Some Borosilicates

J.A. Apps

A request by the Environmental Protection Agency to characterize the fate of a strong sodium borate-sodium hydroxide waste solution containing minor organic constituents when injected into a deep saline aquifer in a sedimentary formation gave rise to an attempt to determine the thermodynamic properties of several borosilicates. The possibility existed that one or more borosilicates might precipitate through interaction of the waste steam with argillaceous sandstones and shales. Borosilicates are also of interest when considering the post-burial hydrothermal alteration of high-level radioactive processing waste, which has been manufactured into borosilicate glass castings. Finally, there is some interest in the possibility that borosilicates may form scale in power plants in which water is treated with sodium borate to control pH and retard corrosion.

Borosilicates are of widespread, though relatively uncommon, occurrence in nature. With the exception of datolite, very little is known about their thermochemical properties. Five borosilicates were chosen for evaluation: axinite, danburite, datolite, dumortierite, and howlite. All but dumortierite contain calcium.

Table 1 summarizes the chemical formulas used in this study; all are based on crystallographic studies. Both dumortierite and axinite are given idealized formulas. In nature, their chemical compositions are variable. Axinite has significant iron and manganese substituted for calcium.

Axinite and datolite are the most frequently observed borosilicates, usually the product of metasomatism of mafic volcanics, and presumably the result of post-consolidation separation and concentration of borate residues in the aqueous phase. Danburite is somewhat less common but is found in a wider range of geothermal environments, including skarns and marine evaporites. With few exceptions dumortierite tends to be restricted to pegmatites, the end result of magmatic crystallization, or to the ini-

Table 1. Structural formulas of borosilicates whose thermodynamic properties are evaluated in this report.

Mineral	Formula	Source
Axinite	$Ca_3Al_2[BO_3][Si_4O_{12}](OH)$	Ito and Takeuchi (1952)
Danburite	$CaB_2Si_2O_8$	Phillips et al. (1974)
Datolite	$CaB[SiO_4](OH)$	Foit et al. (1973)
Dumortierite	$Si_3B[Al_{6.75}\square_{0.25}O_{17.25}(OH)_{0.75}]$	Moore and Araki (1978)
Howlite	$Ca_2SiB_5O_9(OH)_5$	Finney et al. (1970)

tial stages of magmatization. Howlite is found only in marine and saline lake evaporites. Tourmaline was omitted from the evaluation because of its variable composition, which would have necessitated treatment of solid solutions and the introduction of additional chemical components in the system. There is also no evidence that it will form at temperatures below 100°C in the natural environment.

APPROACH TO THE CALCULATION OF THERMODYNAMIC PROPERTIES

To compute the equilibrium relations among minerals over the full range of temperatures, pressures, and bulk compositions found in nature, certain thermodynamic parameters must be known for the participating minerals. These conventionally include the molal volume ($V°$), the entropy at 298 K (S°_{298}), the enthalpy of formation at 298 K ($\Delta H^\circ_{f,298}$), and the variation of heat capacity with temperature ($C^\circ_p(T)$). For consistency with previous studies by Helgeson and his coworkers (e.g., Helgeson et al., 1978), the Maier-Kelley heat-capacity function is used for $C^\circ_p(T)$ (Maier and Kelley, 1932).

Because of the paucity of thermodynamic information on the selected borosilicates, recourse had to be made to iterative approximations using a variety of sources of data. The strategy adopted is as follows:

1. Survey the literature describing the natural occurrences of calcium borosilicates and dumortierite.

2. Summarize the paragenetic associations of the calcium borosilicate minerals and dumortierite with other minerals containing boron, calcium, silicon, and aluminum.

3. Identify natural occurrences where borosilicate minerals coexist. Construct schematic activity diagrams that are topologically compatible with the observed coexistences.

4. Generate quantitative activity diagrams as a function of

$$\log \frac{[Ca^{2+}]}{[H^+]^2} \text{ versus } \log [SiO_2(aq)]$$

at 50°C intervals to 300°C, displaying the stability fields of calcium silicates and calcium aluminosilicates observed to coexist with the selected calcium borosilicates. Estimate the range of log $([Ca^{2+}]/[H]^{2+})$, log $[SiO_2(aq)]$, and log $([Al^{3+}]/[H]^{3+})$, where calcium borosilicates are observed.

5. Calculate the molal volumes ($V°$), entropies (S°_{298}), and heat capacities ($C^\circ_p(T)$) for those borosilicates for which no data currently exist.

6. Utilize all available calorimetric, phase equilibrium, and solubility measurements, together with field observations of paragenetic assemblages, to compute the thermodynamic properties of the calcium borosilicates in sequence.

7. Calculate the solubility products of the borosilicates at 25, 60, 100, 150, 200, 250, and 300°C.

8. Construct activity diagrams as a function of log $[Ca^{2+}]/[H^+]^2$ versus log $[SiO_2$ (aq)] and versus log $[B(OH)_3$ (aq)] at 50° intervals to 300°C to display the stability fields of the borosilicates. Evaluate the stability fields in the context of observed paragenetic associations of borosilicates with each other and with associated minerals, and adjust $\Delta G^\circ_{f(T)}$ of the participating minerals accordingly.

9. Where possible, perform further independent tests of the validity of the computed thermodynamic data.

Although the literature review was not exhaustive, nearly thirty references to the natural occurrences of the selected borosilicate were consulted. Table 2 shows the borosilicate coexistences that were found.

Many of the occurrences of axinite and datolite also included minerals typical of calcium-rich environments, e.g., epidote, zoisite, clinozoisite, grossular, prehnite, wollastonite, vesuvianite, and idocrase. This suggested that an understanding of the stability fields of at least some of these minerals and the temperature ranges over which they were observed to be stable would form a logical basis for estimating the approximate chemical potentials of CaO, Al_2O_3, and SiO_2. Accordingly, activity diagrams for plotting log ($[Ca^{2+}]/[H^+]^2$) versus log $[SiO_2(aq)]$ were constructed at 50°C intervals to 300°C. Figure 1 illustrates the stability relations of the participating members at 250°C. Most of the thermodynamic data used in the computation of the diagram were derived from Haas et al. (1981).

Calorimetric measurements of the thermodynamic properties of the borosilicates are limited to the low-temperature heat-capacity measurements and entropy determinations on danburite and datolite by Agoshkov et al. (1978) and the heat capacity and enthalpy measurements on danburite and datolite by Zhdanov et al. (1978).

Phase-equilibria studies include that by Kurshakova (1975), who determined the temperature and boracic acid content of the coexisting aqueous phase for the divariant reaction

$$\underset{\text{wollastonite}}{CaSiO_3} + B(OH)_3(aq) = \underset{\text{datolite}}{CaB[SiO_4](OH)} + \underset{\text{water}}{H_2O}$$

which permitted her to calculate $\Delta G^\circ_{f,298}$(datolite). Another phase-equilibrium study used in this study is that by Eugster and Wise (1963) on the reaction

$$\underset{\text{datolite}}{2CaB[SiO_4](OH)} + \underset{\text{quartz}}{SiO_2} = \underset{\text{danburite}}{CaB_2Si_2O_8} + \underset{\text{wollastonite}}{CaSiO_3} + \underset{\text{water}}{H_2O}$$

Table 2. Borosilicate mineral coexistences reported in the literature.

Mineral coexistences	No. of observations
Axinite-datolite	5
Axinite-danburite	1
Axinite-dumortierite	1
Danburite-howlite	1
Danburite-datolite-axinite	2(?)

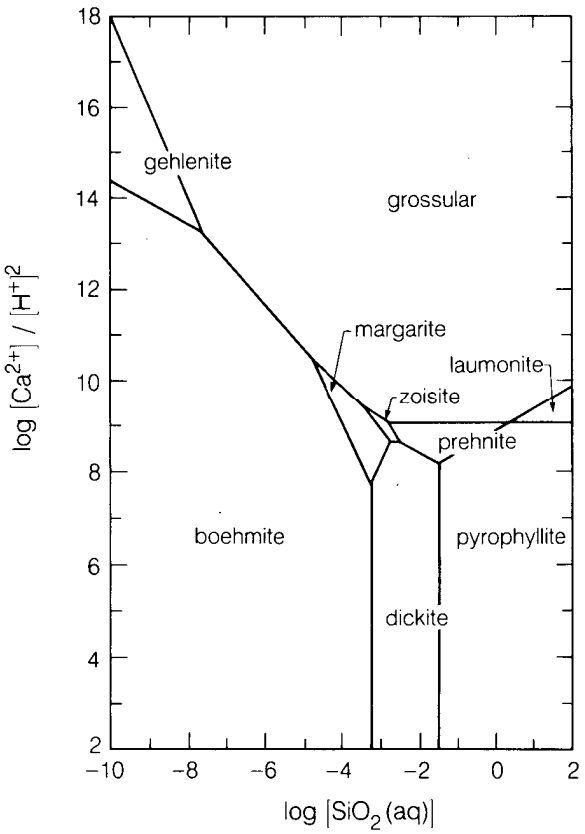

Figure 1. Activity diagram showing part of the system H_2O–CaO–Al_2O_3–SiO_2 at T = 250°C, P = 40 bar. [XBL 883-10102]

The Maier-Kelley heat-capacity functions and entropies of all minerals for which data were not already available were calculated using the empirical equations found by Helgeson et al. (1978) to give reasonable approximations of the correct values. The molal volumes of other minerals were calculated from their mineral densities, rather than from crystallographic data. The methods used in calculating the remaining thermodynamic parameters are summarized in the logic diagram illustrated in Fig. 2. The resulting data are summarized in Table 3.

Difficulties were encountered in reconciling the postulated environmental conditions for the two observed howlite occurrences, i.e., buried playa deposits and marine evaporite deposits. Furthermore, there are conflicting data in the literature for the thermodynamic properties of some of the coexisting sodium, sodium-calcium, and calcium borates, which are required for estimating the solubility of howlite; further study is necessary. A tentative estimate of howlite solubility was established through an assumption that the danburite coexists with quartz

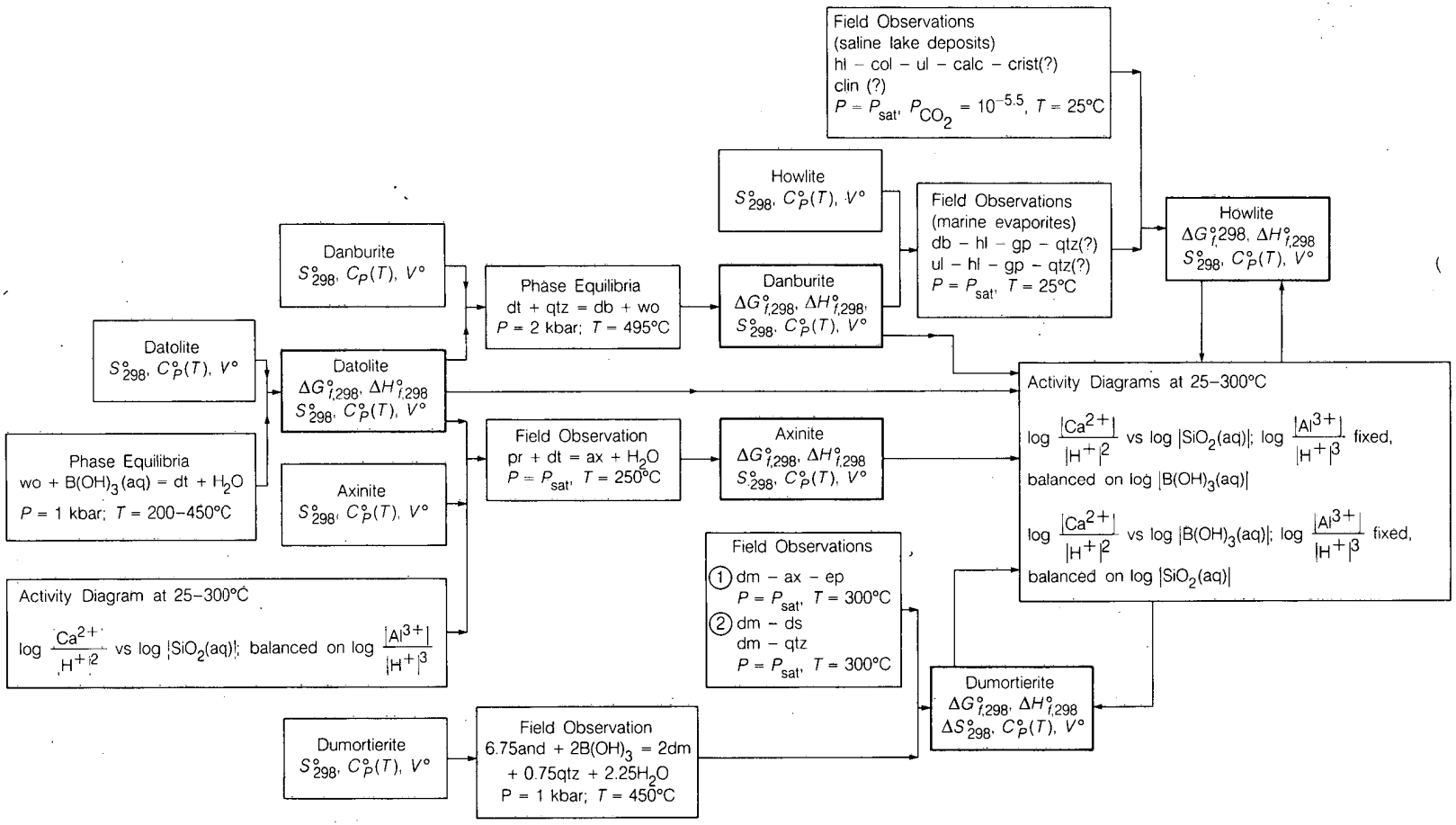

Figure 2. Logic diagram to show the sequence of steps used to calculate the thermodynamic properties of some borosilicates. [XBL 883-10100]

in marine evaporites. Table 3 summarizes all thermodynamic data computed in this study. Calculated solubility products for the borosilicates are given in Table 4. These may be incorporated under certain conditions into the EQ3 code database. The activity diagrams in Fig. 3 display the stability fields of borosilicates calculated at 25°C. These diagrams are generally consistent with field observations and available calorimetric and phase-equilibrium data.

One would be optimistic to suppose that the maximum errors in the computed solubility products do not exceed two log units. Certainly the results of this study should form the basis for designing additional experiments involving phase equilibrium, solubility, and calorimetric measurements from which the thermodynamic properties of borosilicates might be studied further. A more complete discussion of the study is given in Apps et al. (1988), which includes details about the uncertainties in the interpretations and a complete listing of all sources of information used in the computations. Further investigation of the thermodynamic properties of the borosilicates will probably be needed as new information becomes available. For the lastest data, please call (415) 486-5193.

Table 3. Summary of thermodynamic properties of some borosilicates at 298.15 K and 1 bar.

Mineral name	Formula	Gram formula weight (g)	$\Delta G^\circ_{f,298}$ (kcal·gfw^{-1})	$\Delta H^\circ_{f,298}$ (kcal·gfw^{-1})	S°_{298} (cal·gfw^{-1}·K^{-1})	$V^{\circ a}$ (cm^3·gfw^{-1})	$C^\circ_{p,T}$ coefficients		
							a	b × 10^3	c × 10^{-5}
Axinite	$Ca_3Al_2BO_3[Si_4O_{12}](OH)$	554.353	−1882.768	−1997.783	84.89	168.50	119.11	46.06	−27.11
Danburite	$CaB_2Si_2O_8$	245.867	−874.165	−928.063	36.98[b]	81.41	35.57[c]	51.94[c]	−7.48[c]
Datolite	$CaB[SiO_4](OH)$	159.980	−551.000	−589.076	26.33[b]	53.15	34.62[c]	16.48[c]	−7.51[c]
Dumortierite	$Si_3B[Al_{6.75}\square_{0.25}O_{17.25}(OH)_{0.75}]$	565.937	−2066.995	−2196.555	79.08	168.43	137.28	40.29	−39.63
Howlite	$Ca_2SiB_5O_9(OH)_5$	391.327	−1421.930	−1535.876	70.51	151.68	93.21	46.36	−22.07

[a]calculated from measured specific gravity

[b]Agoshkov et al. (1978)

[c]Zhdanov et al. (1978)

Reference reactions used in the computation of S°_{298} and $C^\circ_{p,T}$ Maier-Kelley coefficients.

Axinite

$$\underset{\text{axinite}}{Ca_3Al_2BO_3[Si_4O_{12}](OH)} = \underset{\text{datolite}}{CaB[SiO_4](OH)} + \underset{\text{portlandite}}{2CaO} + \underset{\text{corundum}}{Al_2O_3} + \underset{\text{quartz}}{3SiO_2}.$$

Dumortierite

$$\underset{\text{dumortierite}}{Si_3B[Al_{6.75}\square_{0.25}O_{17.25}(OH)_{0.75}]} + \underset{\text{portlandite}}{CaO} + \underset{\text{structural water}}{0.125\ H_2O} = \underset{\text{datolite}}{CaB[SiO_4](OH)} + \underset{\text{corundum}}{3.375\ Al_2O_3} + \underset{\text{quartz}}{2SiO_2}$$

Howlite

$$\underset{\text{howlite}}{Ca_2SiB_5O_9(OH)_5} + \underset{\text{portlandite}}{3CaO} + \underset{\text{quartz}}{4SiO_2} = \underset{\text{datolite}}{5CaB[SiO_4](OH)}$$

Table 4. Solubility products of borosilicate minerals.

	Log K_{sp} [a]				
T(°C)	Axinite	Danburite	Datolite	Dumortierite	Howlite
0	47.988	4.383	9.216	52.176	22.192
25	42.232	4.428	8.685	41.257	21.362
60	35.427	4.341	8.017	28.378	20.200
100	29.020	4.113	7.343	16.282	18.905
150	23.457	3.712	6.600	3.933	17.339
200	16.255	3.198	5.907	−6.770	15.775
250	11.790	2.621	5.260	−16.065	14.254
300	7.155	1.984	4.624	−24.529	12.777

[a]Solubility reactions are

$Ca_3Al_2BO_3[Si_4O_{12}](OH) + 12H^+ = 2Al^{3+} + B(OH)_3(aq) + 3Ca^{2+} + 4SiO_2(aq) + 5H_2O$

$CaB_2Si_2O_8 + 2H^+ + 2H_2O = 2B(OH)_3(aq) + Ca^{2+} + 2SiO_2(aq)$

$Si_3B[Al_{6.75}\square_{0.25}O_{17.25}(OH)_{0.75}] + 20.25H^+ = 6.75Al^{3+} + B(OH)_3(aq) + 3SiO_2(aq) + 9H_2O$

$Ca_2SiB_5O_9(OH)_5 + 4H^+ + 3H_2O = 5B(OH)_3(aq) + 2Ca^{2+} + SiO_2(aq)$.

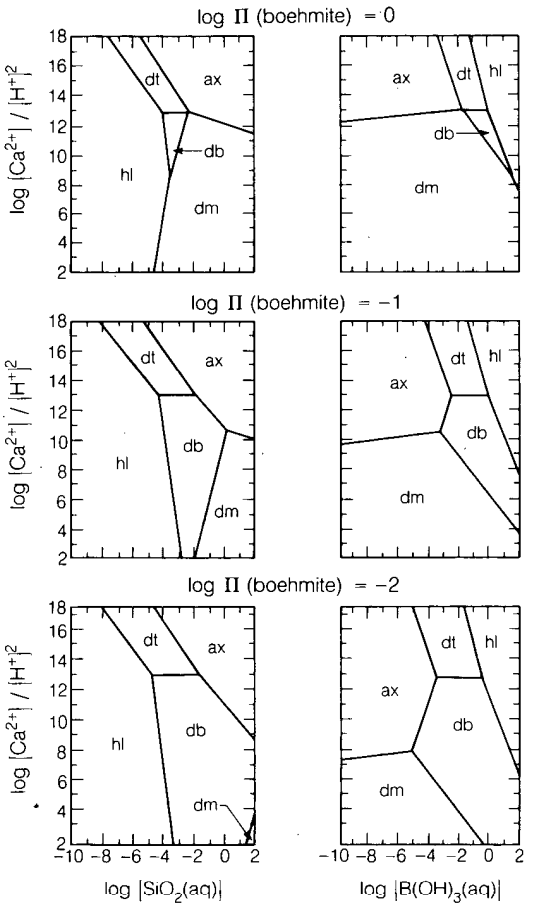

Figure 3. Activity diagrams showing selected borosilicate stability fields in the system H_2O–CaO–B_2O_3–Al_2O_3–SiO_2 at T = 25°C, P = 1 bar. [XBL 883-10101]

ACKNOWLEDGMENTS

The assistance of N. Chuma, N. Lim, and L. Liu in literature searches and data compilation is gratefully acknowledged. Calculations were facilitated through their use of the computer codes DIAGRAM, originally written by Professor T.H. Brown, University of British Columbia, SUPCRT, developed by Professor H.C. Helgeson and his coworkers at the University of California, Berkeley, and EQ3, developed by T.J. Wolery and his coworkers at the Lawrence Livermore National Laboratory.

REFERENCES

Agoshkov, V.M., Semenov, Yu. V., Malinko, S.V., and Khodakovskiy, I.L., 1978. Enthalpies of datolite and danburite between 298.15 and 973.15 K. Geochem. Int., v. 1977, p. 142–147

Apps, J.A., Jun, C.-H., and Chuma, N., 1988. The modeling of the chemical interactions of hazardous waste streams with groundwater and sedimentary host rocks in the injection zones of deep disposal wells. Lawrence Berkeley Laboratory Report LBL-24759 (in preparation).

Eugster, H.P., and Wise, W.S., 1963. Synthesis and stability of datolite and danburite. Schweiz. Mineral. Petrogr. Mitt., v. 43, p. 135–152.

Finney, J.J., Kumbasar, I., Konnert, J.A., and Clark, J.R., 1970. Crystal structure of the calcium silicoborate, howlite. Am. Mineral., v. 55 p. 716–728.

Foit, F.F., Phillips, M.W., and Gibbs, G.V., 1973. A refinement of the crystal structure of datolite, $CaBSiO_4(OH)$. Am. Mineral., v. 58, p. 909–914.

Haas, J.L., Robinson, G.R., Jr., and Hemingway, B.S., 1981. Thermodynamic calculations for selected phases in the system CaO–Al_2O_3–SiO_2–H_2O at 101.325 kPa (1 atm) between 273.15 and 1800 K. J. Phys. Chem. Ref. Data, v. 10, p. 575–635.

Helgeson, H.C., Delany, J.M., Nesbitt, H.W., and Bird, D.K., 1978. Summary and critique of the thermodynamic properties of rock forming minerals. Am. J. Sci., v. 278-A, 229 p.

Ito, T. and Takeuchi, Y., 1942. The crystal structure of axinite. Acta Crystallogr., v. 5, p. 202–208.
Kurshakova, L.P., 1975. Calculations of free energy of datolite formation according to experimental data (in Russian). Geokhimiya, p. 1029–1034
Maier, C.G., and Kelley, K.K., 1932. An equation for the representation of high temperature heat content data. J. Am. Chem. Soc., v. 54, p. 3243–3246
Moore, P.B., and Araki, T., 1978. Dumortierite, $Si_3B[Al_{6.75}\square_{0.25}O_{17.25}(OH)_{0.75}]$: A detailed structure analysis. Neues Jahrb. Mineral., Abh., v. 132, p. 231–241.
Phillips, M.W., Gibbs, G.V., and Ribbe, P.H., 1974. The crystal structure of danburite: A comparison with anorthite, albite and reedmergnerite. Am. Mineral., v. 59, p. 79–85.
Zhdanov, V.M., Turdakin, V.A., Arutyunov, U.S., Semenov, Yu.V., Malinko, S.V., and Khodakovskiy, I.L., 1978. Low temperature specific heat, standard entropy, and elastic parameters of datolite and danburite. Geochem. Int., v. 1977, p. 135– 141.

Thermodynamic Properties of Silicate Materials

I.S.E. Carmichael, V.C. Kress, and D.A. Snyder

Our program continues to focus on the experimental determination of the thermodynamic and physical properties of molten silicates. This past year we have concentrated on redox equilibria in multicomponent silicate liquids and on high-temperature calorimetry. These will be discussed separately.

STOICHIOMETRY OF THE IRON OXIDATION REACTION IN SILICATE MELTS

Iron is unique among the major constituents of natural silicate melts in that it is present in significant portions in more than one oxidation state. The distribution of iron between ferric and ferrous species provides a means by which variations in the chemical potential of oxygen, a quite mobile species, can profoundly influence the structure, rheology, and chemical composition of an evolving magma.

As a first approximation one may consider the oxidation of iron according to the reaction

$$2FeO^{melt} + \frac{1}{2}O_2 = Fe_2O_3^{melt} \qquad (1)$$

from which we may define an equilibrium constant:

$$K_1 \equiv \frac{[a^{melt}_{Fe_2O_3}]}{[a^{melt}_{FeO}]^2 \cdot [f_{O_2}]^{1/2}}, \qquad (2)$$

where a denotes the activity of the subscripted species in the melt phase. Assuming a standard state consisting of the pure component at P and T makes the equilibrium constant K_1 a function of pressure and temperature alone. If one makes the additional assumption that the ferric and ferrous components mix ideally, then a plot of $\ln(X_{Fe_2O_3} / X^2_{FeO})$ (where X_i denotes the mole fraction of the subscripted species i in the melt phase) against $\ln(f_{O_2})$ should be linear, with a slope of one-half. Deviations from such simple behavior will reflect nonideal mixing in ferric and/or ferrous components.

Sack et al. (1980) found that an excellent fit to observations could be obtained using a simple empirical expression of the form

$$\ln\left(\frac{X^{liq}_{Fe_2O_3}}{X^{liq}_{FeO}}\right) = a \ln f_{O_2} + \frac{b}{T} + c + \sum_i d_i X_i \,, \qquad (3)$$

where a, b, and d_i are regression coefficients and the sum is over the oxide components i. Kilinc et al. (1983) refined the compositional parameters d_i by supplementing the data base of Sack et al. (1980) with 46 additional experiments (in air) on compositions ranging from those of nephelinite to rhyolite.

Recent high-precision determinations of the ferric/ferrous distribution in mid-ocean ridge basalt (MORB) glasses (Christie et al., 1986) suggest that submarine basalts equilibrate under far more reducing conditions than had been previously believed. Using reaction (3) with the regression coefficients of Kilinc et al. (1983), Christie et al. (1986) estimated quench oxygen fugacities up to 3 $\log_{10}$ units below the nickel-nickel oxide (NNO) oxygen buffer. These